

# A new practical model to describe Moisture Ratio behavior during drying process

López-Ortiz, A.<sup>1</sup> | Reyna-Guillén, J.<sup>1\*</sup> | Wong-Loya, J.A.

<sup>1\*</sup>

<sup>1</sup>Instituto de Energías Renovables,  
Universidad Nacional Autónoma de México,  
Temixco, Morelos, 62580, México

**Correspondence**

Wong-Loya, J.A.  
Email: jawol@ier.unam.mx

**Funding information**

Funder One, Funder One Department,  
Grant/Award Number: 123456, 123457  
and 123458; Funder Two, Funder Two  
Department, Grant/Award Number:  
123459

A new mathematical model has been developed to analyze the process of drying food. The model is based on a non-linear function fit of the moisture ratio behavior. To determine the moisture ratio behavior, the Rational Polynomial method of first and second order has been proposed, which allows a simple fit that approximately describes the moisture ratio behavior. The Pearson coefficients obtained for the fitted series were greater than 0.9948. The fitting process has been automated using a simple Wolfram language script. This model has been compared against the most commonly used models and applied to a set of 39 experimental data series. The RP method for the second order showed good agreement in 82.05% of the analyzed series and was the best fit in 61.5% of all the data sets. On the other hand, the first order showed good agreement in only 30.77% of the analyzed series.

**KEYWORDS**

Rational polynomial functions, *Mathematical modeling*, Food drying, Solar drying

---

\* Equally contributing authors.

## 1 | INTRODUCTION

Every year, the world generates approximately 1.3 billion tons of food losses and waste, according to a report by [1]. It is crucial to adopt food preservation methods that are both environmentally friendly and effective. Drying is one of the most commonly used methods in the food industry to prevent post-harvest losses and quality degradation [2]. By reducing the moisture content of products, drying helps to maintain microbial stability and extend their shelf-life. This method achieves this by reducing enzymatic and oxidative degradation, thereby preserving the quality of the food product. The benefits of drying make it a popular choice for food preservation in the industry, as highlighted in a study by [3].

Among them, drying is an important option that can reduce the weight of the product, and broaden product availability. Therefore, dried products with prolonged shelf life become available all year round and can be shipped over long distances [4]. Furthermore, different drying techniques are implemented to improve drying time and food quality [5, 6, 7, 8]. Nowadays, dried products are popular with consumers as a result that they are very convenient in our busy lives. The increasing number of shoppers represents a challenge for food manufacturers to develop options for diversifying and accelerating food production. Therefore, in the food industry, fruits and vegetables are generally processed by drying [9, 10].

Drying is a unit operation that promotes moisture content migration from cellular structures to pores, surfaces, and surroundings. Moisture migration involves coupled heat and mass transfer phenomena [11] due to temperature gradient, pressure gradient, and moisture content gradient. The necessity to design and build new optimized drying systems leads to different research work. Therefore, models to explain adequately the influence of external and internal conditions on drying time and drying characteristics are necessary. External conditions, such as the temperature and relative humidity of the air, air velocity, and pressure are the most influential variables during drying [12, 13].

Additionally, internal conditions such as characteristic macroscopic and microscopic structure are considered in modeling but imply a very complex mathematical and numerical solution. Therefore, a simplified system of two components (solid and water) is usually used.

Theoretical, empirical, and semi-empirical drying predictive models derived from Newton's law of cooling and Fick's second law have been proposed in the available literature [14, 15, 16, 17, 18]. In general, moisture migration can occur by liquid diffusion, vapor diffusion, Knudsen diffusion, diffusion on the surface, differences of hydrostatic pressures, or a combination of them [19].

Although there are several methods to analyze the behavior of relative moisture content (MR) during the drying process, these have not been able to adequately fit most of the analyzed cases. For example, in solar drying or a system that uses non-isothermal conditions for air drying, the models do not have a good fitting for experimental values due to the changing drying conditions. So, the development of methods is still a task to work on.

Therefore the objective of this study is to develop a new practical method based on a rational polynomial function which was used to describe the relative moisture behavior during the drying food process, which is an important task for the appropriate drying kinetic description and modeling in process under changing processing conditions.

### 1.1 | Drying kinetics

Normalized drying kinetic is usually represented using the dimensionless moisture content or moisture ratio (MR) as represented in equation 1.

$$MR = \frac{(X - X_e)}{(X_0 - X_e)} \tag{1}$$

where X is the moisture content of the sample at any drying time. X<sub>0</sub> is the initial moisture content, and X<sub>e</sub> is the equilibrium moisture content. In many experiments, the final recorded weight is used for the X<sub>e</sub> calculation.

At the beginning of drying, when t=0, the moisture content X=X<sub>0</sub>. When drying ends X=X<sub>e</sub>, then, the last data in normalized drying kinetics should be 0.

### 1.2 | Models commonly used to describe drying kinetics

Simulation models of drying processes are used to design new drying systems or improve existing ones [20].

Thin-layer drying equations are fundamental to drying simulation. These represent the equations for moisture exchange between a thin layer of drying product and the surrounding air. From a mathematical point of view, a thin layer represents the infinitesimally small chosen spatial dx within which air humidity and temperature changes can be assumed linear [20, 21].

Thin-layer drying machines have recently been found to have wide application due to their ease of use and less data requirements, unlike complex distributed models (such as phenomenological and coagulation coefficients) [22].

Different methods have been developed, both theoretical and empirical, to study the behavior of the amount of moisture, in this study we used the most common used methods to describe the moisture ratio behavior (see table 1). These methods are analogous to Newton's law of cooling, derived from Fick's second law of diffusion, and also in empirical models that can be found in the literature [14, 15, 16, 17, 18, 23, 24].

**TABLE 1** Description of the most commonly used model for drying processes

	Name	Equations
Models analogues to		
Newton's Law of cooling	Lewis (L)	$MR = \exp(-kt)$
	Page (P)	$MR = \exp(-kt^n)$
Models resulting from		
Fick's second law of diffusion	Henderson and Pabis (HP)	$MR = a \exp(-kt)$
	Logarithmic (Log)	$MR = a \exp(-kt) + c$
	Two-term (TT)	$MR = a \exp(-kt) + b \exp(-k_1t)$
	Two-term Exponential (TTE)	$MR = a \exp(-kt) + (1 - a) \exp(-k_1t)$
	Midilli and Kucuk (MK)	$MR = a \exp(-kt^n) + bt$
Empirical model	Wang and Sighn (WS)	$MR = 1 + at + bt^2$

## 2 | RATIONAL POLYNOMIAL METHOD (RP) DEVELOPMENT

In engineering and science, physicochemical and thermodynamic processes may be described (physically and mathematically) through typical asymptotic behaviors, Relative moisture content behavior during the drying process can be modeled using rational polynomial functions.

Under such conditions, several mathematical functions could fit the resulting asymptotic trends. One of these functions is the well-known RP function, which has been successfully used in a wide variety of engineering applications for modeling experimental data that exhibit an asymptotic trend e.g. [25, 26, 27, 28, 29, 30, 31, 32] The RP function is based on the well-known Pade approximation [33], such an approximation is an RP function that could be proposed as a generalization of the Taylor polynomial model, where the mathematical function is given by the ratio of two polynomials.

The generalized equation of an RP function is given by the following mathematical expression (eq. 2):

$$y(x) = \frac{p_0 + p_1 x^2 + \dots + p_k x^k}{q_0 + q_1 x^2 + \dots + q_j x^j} \quad (2)$$

The coefficients  $p_i$  and  $q_i$ , (from  $i = 0, 1, 2, \dots, k$ , and  $j = 0, 1, 2, \dots, j$  respectively) in equation (eq. 2) may have distinct specifications, leading to different approaches, and may be integer coefficients or fractions.

To obtain the  $y$  values at their corresponding  $x$  data, it is therefore necessary to determine numerically the coefficients  $p_i$  and  $q_i$ .

For this particular application, the dependent variable ( $y$ ) has been defined by the  $MR$  measurements, whereas the independent variable ( $x$ ) was given by the drying time. After applying the mathematical fundamentals of the RP function, a  $q_0$  coefficient with a value of 1 was proposed, to avoid indetermination in the model

$$MR = \frac{p_0 + p_1 t + \dots + p_k t^k}{1 + q_1 t + \dots + q_j t^j} \quad (3)$$

According to equation (eq. 3), the total number of coefficients will be given by the following sum:  $n = k + j + 1$ . Thus,  $n$ -pairs of data ( $t$ ,  $MR$ ) are required to obtain  $n$ -  $n$ -equations, which must be numerically solved to determine their coefficients [33].

To solve the asymptotic trends exhibited relative moisture measurements  $MR(t)$  during the drying process (see Fig 1), RP functions of first and second degree should be proposed for fitting the  $MR$  data sets.

This mathematical condition implied that the highest  $k$  and  $j$  exponents of the RP functions adopt values equal to 1 and 2. Equation (eq. 3) was therefore reduced to two mathematical functions (eqs. 4 and 5) which directly depend on the polynomial-degree:

$$MR = \frac{p_0 + p_1 t}{1 + q_1 t} \quad (4)$$

$$MR = \frac{p_0 + p_1 t + p_2 t^2}{1 + q_1 t + q_2 t^2} \quad (5)$$

Equations (eqs. 4 and 5) can be used to fit several experimental datasets using the least square methods and is the base of the method proposed here. From here, we will call this mathematical model the Rational Polynomial Method (RP) for the first order (eq. 4), and second order (eq. 5) will be referred to as FO and SO respectively.

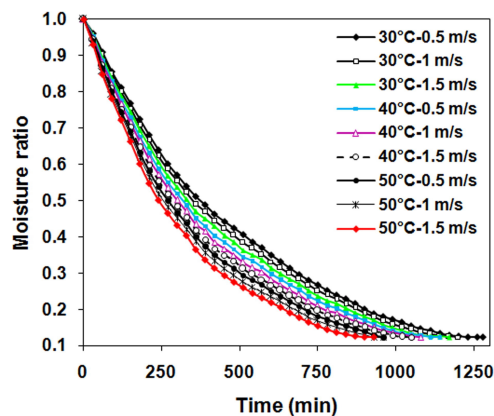


FIGURE 1 Moisture ratio behavior of peppermint leaves. Taken from [34]

3 | METHODOLOGY

For the development of this work, the methodology presented in the following flowchart (see figure 2) was proposed, which is explained in detail subsequently.

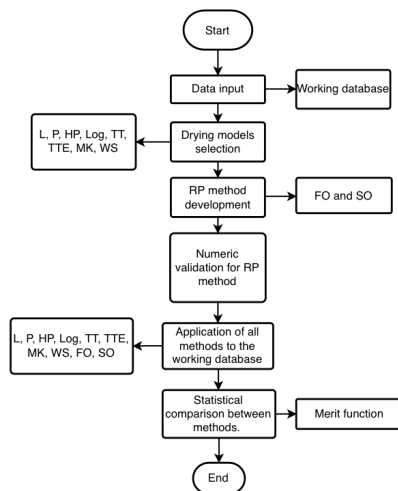


FIGURE 2 Methodology flowchart

- a) Creation of a working database collected from different research and experimental works.
- b) Selection of methods commonly used in the literature for modeling moisture content like Newton's Law of cooling: Lewis and Page; the models resulting from Fick's second law of diffusion: Henderson and Pabis, Logarithmic, Two-term, Two-term exponential, and Midilli and Kucuck as well as the empirical model of Wang and Singh.
- c) Development of RP method.
- d) Apply the RP method for first and second order (eq. 4 and 5) respectively to the working database.
- e) Comparison between the experimental data and the RP method for first and second order.
- f) Comparison between the RP method for first and second order versus the most commonly used models for moisture content.
- g) Determine the applicability and accuracy of the RP method through merit function.

### 3.1 | Working database

Drying data were collected from different research and experimental works. Distinct dryers were used in each experiment and different drying conditions and pre-treatments were applied in each case.

#### 3.1.1 | Convective loop tray dryer experiments

This experiment was previously described by López-Ortiz [35, 13]. A convective loop tray dryer (Patent MXPA06008850) was used for sliced garlic (*Allium sativum*, L.) drying (Fig. 3). Three different temperatures were tested 40, 50, and 60°C.



**FIGURE 3** Convective loop tray dryer used in garlic drying

#### 3.1.2 | Greenhouse dryer experiments

The greenhouse solar dryer (GSD) was previously described by Román-Roldan[36]. The GSD was connected to three solar collectors for air heating (Fig. 4). Nufar Basil leaves (*Ocimum basilicum*) cultivated in Tequesquitengo, Morelos, Mexico were used for the drying process. Only the leaves were used and placed one by one in the trays. An area of 16 m<sup>2</sup> was used for the trays.

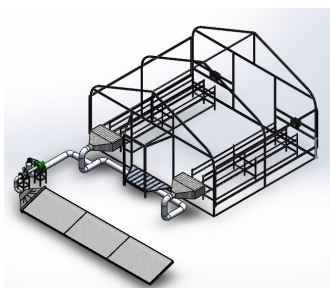


**FIGURE 4** Solar greenhouse dryer (GHD), view without plastic cover and with air solar heaters.

### 3.1.3 | Cabinet solar dryer experiments

The cabinet solar dryer (Fig. 5) was previously described by [37] and was used for experiments with strawberries. Commercial ripening strawberries (*Fragaria vesca*) were sliced (2mm) and coated with different water solutions for solar irradiance protection. The coating was made by immersion for 3 seconds. Five water solutions with bio-polymers were tested. Nopal mucilage (M-N), fenugreek mucilage (FENO), xanthan (G-X), Arabic (G-A), and guar (G-G) gums were used. the coated samples were placed in plastic meshes and introduced in the solar dryer. All experiments were made simultaneously.

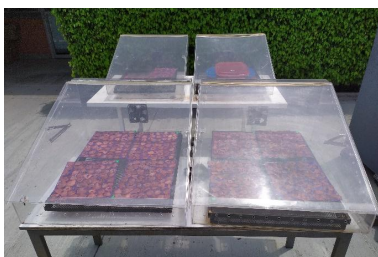


**FIGURE 5** Cabinet-type direct dryer system used in experiments with coated and without coating strawberry slices

### 3.1.4 | UV-blue filtered solar drying experiments

The UV-blue solar filter used as a covering material in drying (Fig. 6) was previously described by [38]. We used commercial frozen products from the local market. Strawberries and blackberries were blended separately. The obtained pulps were transferred into the 35x50x0.5 cm plastic trays. The pulp thickness average was  $3 \pm \text{mm}$ . Four trays were occupied: two for direct drying in the sun and two for drying with a filter.

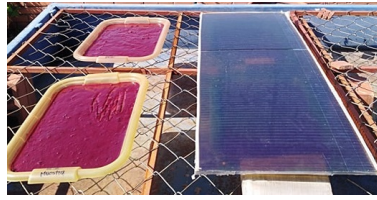


**FIGURE 6** Solar drying with UV-Blue light filter and without filter.

### 3.2 | Database description

As a result of the experiments mentioned above, a working database was created. This database has 39 series described below.

**TABLE 2** Description of the data series utilized

Data series (Series number)	Description (Type of food)
AJ1-AJ6	Sliced garlic ( <i>Allium sativum</i> , L)
AB1-AB5	Nufar Basil Leaves. ( <i>Ocimum basilicum</i> )
ZR1 - ZR6	Blended blackberries ( <i>Rubus</i> )
FR1-FR22	Blended Strawberries ( <i>Fragaria vesca</i> )

### 3.3 | Application of the RP method to the data sets.

To efficiently apply the RP method, a simple computer script in Wolfram Language was created; this script can be requested from the corresponding author.

The database was imported to the Wolfram program *Mathematica*, then a nonlinear model fit was requested to apply the FO (eq.4) and the SO (eq. 5) models to the 39 data series summarized in table 2. After verifying that the data matched the models, we moved on to comparing them.

### 3.4 | Comparison of the experimental data to the methods

It's proposed to use a merit function to quantitatively measure the correlation between the FO and SO models and the drying data.

$$N = \sqrt{\frac{\sum_{t_i}^{t_f} (E(t) - M(t))^2}{\sum_{t_i}^{t_f} E(t)^2}} \quad (6)$$



Where  $E(t)$  is the experimental data,  $M(t)$  is the calculated data. Concerning having a good fit, it is expected to obtain a value close to zero. This merit function has been used to show the agreement between the experimental and simulated data [39, 40, 32].

Finally, to analyze the applicability of the RP method, it was compared with the methods that are commonly used to analyze drying data (Lewis, Page, Henderson and Pabis, Logarithmic, Two-term, Two-term exponential and Wang and Singh model) by applying all of the methods to the same working database and then using the merit function.

An  $N$  value less than the median value of all the  $N$  values obtained was considered as the value for an acceptable agreement of the methods, and the method with the smallest  $N$  value has the best concordance with the dataset analyzed.

## 4 | RESULTS AND DISCUSSION

### 4.1 | RP method application

This study presents the development of a new methodology for analyzing the food drying process. The proposed method is based on a rational polynomial function fit of the moisture ratio behavior, which allows for a simple and practical analytical relation. The accuracy of the model was evaluated by applying it to 39 datasets and comparing it against the most commonly used methods, resulting in better results. This approach aims to provide a self-consistent and practical way to formulate equations that describe the food drying process through the moisture ratio.

To demonstrate the applicability of the RP method for both first and second order, we selected six series from the 39 analyzed. These six series were chosen based on their different RP fit cases, including good agreement (Fig. 8a and 8b) a regular agreement (Fig. 8c and 8d) and poor agreement (Fig. 8e and 8f ).

#### 4.1.1 | Nufar Basil Series (AB1 and AB2)

This dataset contains 16 pairs of Moisture Ratio vs Time for Nufar Basil leaves, with drying time ranging from 0 to 329 minutes in a greenhouse dryer experiment.

The moisture ratio behavior of the AB1 and AB2 series can be represented by the mathematical models obtained through the RP method for the first (FO) and second (SO) orders. The equations 7 and 7 correspond to the FO model for AB1 series, while equations 10 and 10 represent the SO model for AB2 series.

#### | AB1

$$MR(t)_{FO} = \frac{1.10161 - 0.0036984t}{1 + 0.00461791t} \quad (7)$$

$$MR(t)_{SO} = \frac{0.993941 + 0.003691101t - 0.0000186805t^2}{1 + 0.00041097t + 0.000137042t^2} \quad (8)$$

## AB2

$$MR(t)_{FO} = \frac{1.09175 - 0.00388304t}{1 + 0.00573752t} \quad (9)$$

$$MR(t)_{SO} = \frac{0.9999999 - 6.35846 \times 10^7 t + 220852.9527t^2}{1 - 4.913804 \times 10^7 t - 473626.13557t^2} \quad (10)$$

Table 3 shows the calculated fitting results by applying eq. 7 and 8 for AB1 series and 9 and 10 for the AB2 series.

**TABLE 3** Results obtained by applying the FO and SO models to the AB1 and AB2 series. The Moisture Ratio is dimensionless.

AB1						AB2				
Time [min]	Moisture Ratio	FO Model	ADV	SO Model	ADV	Moisture Ratio	FO Model	ADV	SO Model	ADV
0	1.0000	1.1016	0.1016	0.9939	0.0061	1	1.0917	0.0917	1.0000	7.45E-09
20	0.9903	0.9408	0.0495	0.9974	0.0071	0.9745	0.9097	0.0648	1.0095	0.0350
37	0.8984	0.8240	0.0745	0.9186	0.0202	0.8498	0.7821	0.0678	0.8313	0.0186
60	0.7864	0.6888	0.0976	0.7564	0.0300	0.6892	0.6388	0.0503	0.6490	0.0402
82	0.6654	0.5791	0.0864	0.5989	0.0665	0.5578	0.5259	0.0319	0.5169	0.0409
103	0.3779	0.4884	0.1105	0.4711	0.0932	0.3964	0.4348	0.0384	0.4170	0.0206
126	0.3181	0.4018	0.0837	0.3602	0.0420	0.3423	0.3497	0.0073	0.3286	0.0137
149	0.2913	0.3261	0.0349	0.2752	0.0161	0.2327	0.2767	0.0439	0.2563	0.0235
171	0.2427	0.2622	0.0194	0.2125	0.0302	0.1877	0.2159	0.0282	0.1984	0.0107
192	0.1748	0.2075	0.0328	0.1654	0.0094	0.0991	0.1647	0.0656	0.1512	0.0521
214	0.1397	0.1560	0.0163	0.1261	0.0136	0.0676	0.1171	0.0495	0.1085	0.0409
236	0.1322	0.1095	0.0227	0.0945	0.0377	0.0571	0.0745	0.0174	0.0712	0.0142
257	0.0695	0.0691	0.0004	0.0698	0.0003	0.0428	0.0379	0.0049	0.0399	0.0028
280	0.0284	0.0288	0.0004	0.0475	0.0191	0.0195	0.0017	0.0178	0.0096	0.0099
305	0.0119	-0.0110	0.0229	0.0275	0.0156	0.0068	-0.0337	0.0404	-0.0195	0.0263
329	0.0000	-0.0457	0.0457	0.0117	0.0117	0	-0.0643	0.0643	-0.0443	0.0443

ADV is the absolute difference value

## 4.2 | Blended Strawberries.

The FR20 series comes from the UV-blue filtered solar drying experiments, using a filter and the strawberry pulp. The FR7 series is obtained from the Cabinet solar dryer experiments, using commercial strawberries sliced into 2mm and coated with the FENO solution. Finally, series FR12 was acquired from the cabinet solar dryer experiments, using sliced strawberries and coated into the (M-N) solution. The series is composed of 9 data pairs, and the drying time range proceeds from 0 to 360 minutes.

The mathematical models obtained by applying the RP method for the first (FO) and second (SO) order are presented in (eqs. 11 and 12) respectively for FR7 series, (eqs. 13 and 14) for FR12 series, and (eqs. 15 and 16) for FR20 series which represent moisture ratio behavior.

## FR7

$$MR(t)_{FO} = \frac{1.018846 - 0.00422018t}{1 + 0.0192256t} \quad (11)$$

$$MR(t)_{SO} = \frac{0.992087 - 0.00881606t + 0.000017777t^2}{1 - 0.00382149t + 0.0000433676t^2} \quad (12)$$

## FR12

$$MR(t)_{FO} = \frac{1.0476 - 0.00411087t}{1 + 0.0111891t} \quad (13)$$

$$MR(t)_{SO} = \frac{0.984427 - 0.00887638t + 0.0000182629t^2}{1 - 0.00454126t + 0.0000562203t^2} \quad (14)$$

## FR20

$$MR(t)_{FO} = \frac{0.998255 - 0.00286537t}{1 + 0.00260401t} \quad (15)$$

$$MR(t)_{SO} = \frac{0.9999999 - 30.231t - 0.0868799t^2}{1 - 30.4217t - 0.0771963t^2} \quad (16)$$

Table 4 shows the results derived from reproducing the model obtained above and applying them to the series FR7, FR12, and FR20.

**TABLE 4** Results obtained by applying the FO and SO models to the FR7, FR12, and FR20 series. The Moisture Ratio is dimensionless.

FR7						FR12					FR20				
Time [min]	Moisture Ratio	FO Model	ADV	SO Model	ADV	Moisture Ratio	FO Model	ADV	SO Model	ADV	Moisture Ratio	FO Model	ADV	SO Model	ADV
0	1	1.0188	0.0188	0.9921	0.0079	1	1.0476	0.0476	0.9844	0.0156	1	0.9983	0.0017	1.0000	6.60E-07
30	0.6158	0.5659	0.0500	0.6446	0.0287	0.7738	0.6920	0.0818	0.8034	0.0296	0.8489	0.8462	0.0028	0.8440	0.0050
60	0.3958	0.3555	0.0403	0.3805	0.0153	0.5463	0.4792	0.0671	0.5566	0.0103	0.6969	0.7147	0.0178	0.7139	0.0170
90	0.2689	0.2340	0.0349	0.2021	0.0668	0.4121	0.3376	0.0744	0.3186	0.0934	0.5970	0.5998	0.0028	0.5999	0.0029
120	0.0070	0.1549	0.1480	0.0913	0.0843	0.0497	0.2366	0.1869	0.1441	0.0944	0.5340	0.4986	0.0354	0.4992	0.0349
180	0.0012	0.0581	0.0570	-0.0061	0.0072	0.0012	0.1021	0.1008	-0.0108	0.0120	0.2976	0.3285	0.0309	0.3294	0.0317
240	0	0.0011	0.0011	-0.0226	0.0226	0	0.0166	0.0166	-0.0298	0.0298	0.2226	0.1911	0.0315	0.1917	0.0309
300	0	-0.0365	0.0365	-0.0087	0.0087	0	-0.0426	0.0426	-0.0074	0.0074	0.0408	0.0778	0.0370	0.0778	0.0370
360	0	-0.0632	0.0632	0.0153	0.0153	0	-0.0860	0.0860	0.0234	0.0234	0	-0.0172	0.0172	-0.0179	0.0179

### 4.2.1 | Blended blackberries.

The ZR1 series were acquired from the UV-blue filtered solar drying experiments, using a filter. This series comprises 11 data pairs with a drying time range from 0 to 480 minutes.

The mathematical expression obtained by applying the RP method for the FO and SO models is shown in (eqs. 17 and 18) respectively.

$$MR(t)_{FO} = \frac{1.08228 - 0.0025535t}{1 + 0.00262667t} \quad (17)$$

$$MR(t)_{SO} = \frac{0.994804 - 0.000112429t - 4.27737 \times 10^{-6}t^2}{1 - 0.000701912t + 0.0000418089t^2} \quad (18)$$

These models were used to reproduce the ZR1 series, table 5 presents the calculated values for each model as well as the experimental data.

**TABLE 5** Results gotten by applying the FO and SO models to the ZR1 series.

Time [min]	Moisture Ratio	FO Model	ADV	SO Model	ADV
0	1	1.0823	0.0823	0.9948	0.0052
30	0.9691	0.9322	0.0369	0.9715	0.0024
60	0.8702	0.8025	0.0677	0.8775	0.0074
90	0.7470	0.6893	0.0577	0.7448	0.0022
120	0.6272	0.5897	0.0375	0.6059	0.0213
180	0.3438	0.4225	0.0787	0.3752	0.0314
240	0.2330	0.2877	0.0547	0.2227	0.0103
300	0.1322	0.1765	0.0444	0.1266	0.0056
360	0.0751	0.0834	0.0083	0.0649	0.0103
420	0.0090	0.0043	0.0047	0.0239	0.0149
480	0	-0.0638	0.0638	-0.0043	0.0043

### 4.2.2 | Statistical results

Table 6 shows the summary of statistical values such as the merit function obtained, the maximum absolute difference value between the experimental data and the predicted, and the determination coefficients obtained by applying the RP method to the six series shown above.

**TABLE 6** Results obtained by applying the FO and SO models to the AB1 and AB2 series. The Moisture Ratio is dimensionless.

	$N_{FO}$	$ADV_{FO}$	$R^2_{FO}$	$N_{SO}$	$ADV_{SO}$	$R^2_{SO}$
AB1	0.1185	0.1105	0.9692	0.0679	0.0932	0.9899
AB2	0.9997	0.0917	0.9803	0.0592	0.0052	0.993
FR7	0.1499	0.148	0.94648	0.0918	0.0843	0.9868
FR12	0.1885	0.1869	0.9391	0.0995	0.0944	0.983
FR20	0.0417	0.037	0.9948	0.0416	0.037	0.9948
ZR1	0.0923	0.0823	0.9791	0.0225	0.0314	0.9987

ADV is the maximum absolute difference value gotten in that series.

### 4.3 | Methods comparison

To compare the results, the proposed method and the most commonly used models (Lewis, Page, Henderson and Pabis, Logarithmic, Two-term, Two-term exponential, and Wang and Singh models) were applied to the data series. The values for the merit function (eq. 6) were calculated for each method to determine the fit agreement with the data series as well as the squared correlation coefficient.

To determine whether a method had a good agreement, an arbitrary parameter was proposed, which was the median of all the merit function values ( $N_m$ ); because the distribution of the N values was not normal, the median was an adequate parameter [32]. The median calculated N value was  $N_m = 0.07382$ .

A comparison of the methods applied to the six series described above was performed. The fitting results of all the models used are shown in.

**TABLE 7** Summary of the application of the 9 fitting models to the 39 data series.

Method	Number of good agreements	Number of best fit	N-value median
Henderson and Pabis	11	0	0.09593
Logarithmic	19	5	0.07626
Midilli and Kucuck	17	1	0.08192
Lewis	10	0	0.10829
First Order	12	0	0.09515
Second Order	32	24	0.04169
Two-term	30	4	0.05274
Two-term Exponential	31	0	0.05222
Wang and Sighn	8	0	0.12431
Page	22	5	0.05699
Median of all N-Values			0.07382

A complete comparison was performed using all 39 series and is presented in detail and shown in Table 7 con-

taining the results of the application and comparison against the most commonly used methods. After applying the methods to the 39 data series, the results indicate: a) The Wang method was the poorest agreement, just having 8 good agreements of all series and none of them had the best fit, b) the Lewis, Henderson and Pabis and First Order have several good agreements of 10, 11 and 12 respectively and none of them was the best fit, c) the Midilli and Kucuck, Logarithmic and Page methods have a regular agreement, with several good agreements of 17, 19 and 22 respectively, and they were the best fit in 1 series for the MK method and in 5 series for the Log and P method and d) the Two-term, Two-term Exponential and Second order have a good fitting with some good agreements of 30, 31 and 32 respectively in all the 39 series, also the Two-term exponential method was the best fit for 4 series and the Second Order was for 24 series out of 39. The method that showed the best results was the SO model, which had good agreement with 32 series and was the best fit for 24 data series. The results are shown in Fig. 7, where the N value calculated for each method in all datasets line shows good agreement with the dataset.

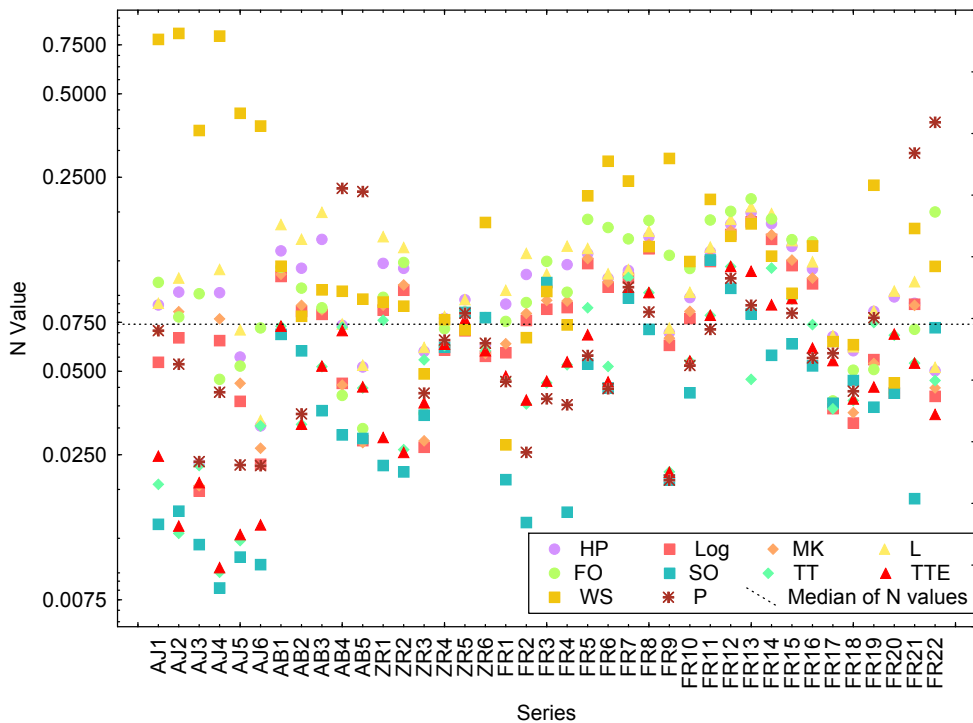
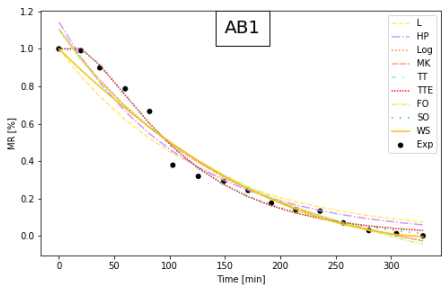
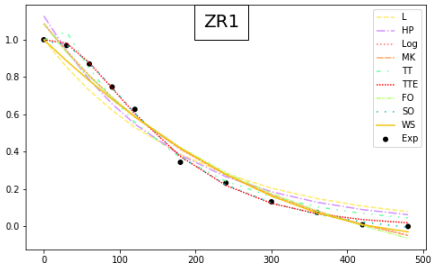


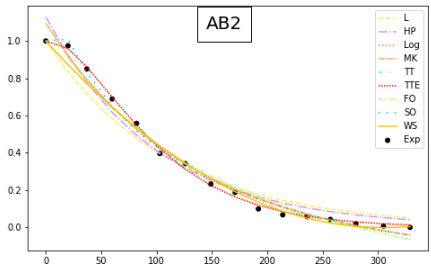
**FIGURE 7** Results of applying the 9 methods (Second Order, First Order, Lewis, Page, Modified Page, Henderson and Pabis, Logarithmic, Two-term, Two-term exponential, Midilli and Kucuck and Wang and Singh models) to the 39 data series.



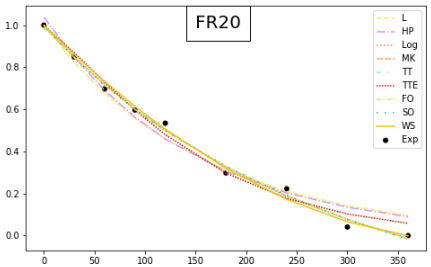
(a) AB1 Series



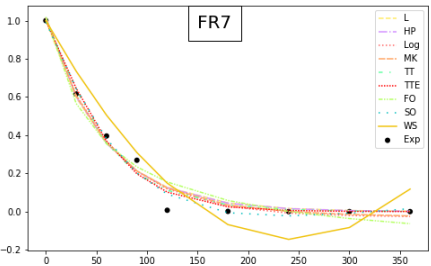
(b) ZR1 series



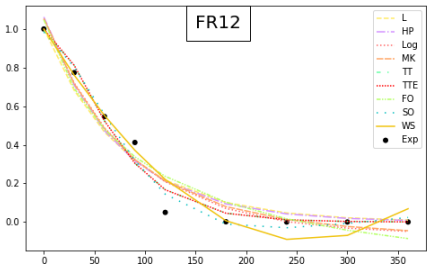
(c) AB2 series



(d) FR20 series



(e) FR7 series



(f) FR12 series

**FIGURE 8** Comparison of the 9 models using the series AB1, ZR1, AB2, FR20, FR7 and FR12

Analyzing the 39 series, the RP method for the Second Order model has a good agreement in 82.05% of the analyzed series, the TTE method has a good fitting in 79.49% of the analyzed series, the TT model has a good agreement in 76.92% of the analyzed series, the P method has a good fitting in 56.41% of the analyzed series, the Log method has a good fitting in 48.72% of the analyzed series, the MK method has a good fitting in 43.59% of the analyzed series, the FO method has a good agreement in 30.77% of the series analyzed, the HP method has a 28.21% of good fitting in the series analyzed, the L method has a good agreement of 25.64% in the series analyzed and finally the WS method has a 20.51% of good fitting in the series analyzed as presented in figure 9.

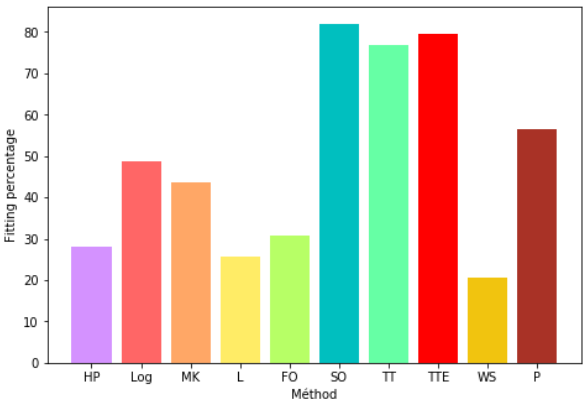


**FIGURE 9** Probability of having a good fit by method

Regarding the best-fit method for each series; the SO method was the best-fit model for 61.54% of the series, the Page method was the best-fit model for 12.82% of the series, the Logarithmic model was the best fit for 12.82% of the series, the Two-term was the best-fit model for 10.26% of the series, the Midilli and Kucuck was the best-fit model for 2.56% of the series and finally the Henderson and Pabis, Lewis, First Order, Two-term Exponential and Wang and Sighn models were not the best-fit model for any of the analyzed series.

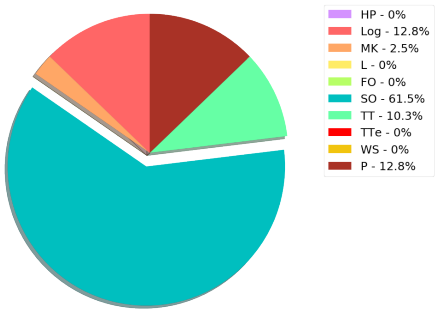


**FIGURE 10** The best fit by method



## 5 | CONCLUSIONS

A new practical method was successfully developed to describe the moisture ratio behavior of drying food. The new method is based on the use of the rational polynomial function to model the moisture ratio behavior. A Wolfram language script was developed for the application of the RP method. The applicability of nine methods (including the RP for first and second order) was evaluated in 39 data series, where the SO model had the best agreement in 32 series over the Henderson and Pabis, Logarithmic, Midilli and Kucuk, Lewis, First Order, Two-term, Two-term Exponential, Wang and Sighn and Page methods, which are commonly used methods to describe the moisture ratio behavior, as well as the SO model was the best-fit model in 24 series of the data sets analyzed. The new RP method for second order and the Wolfram language script allow fitting the moisture ratio behavior of different foods, which constitutes a competitive advantage over the analytical and empirical methods currently available for drying food industries. Finally, the future application of this new practical method by the drying food industries will optimize the drying food process.

## acknowledgements

The authors want to thank UNAM and the IPN for their infrastructure. Partial financial support was received under **Project PAPPIT TA200320** and **PAPIME PE110319** as well as Navarrete Salgado, M and Pacheco Pineda I.Y. for their support in performing the experiments.

## references

- [1] Gustavsson J, Cederberg C, Sonesson U, van Otterdijk R, Meybeck A. Food and Agriculture Organization of the United Nations. Global Food Losses and Food Waste.; 2011.
- [2] Menon A, Stojceska V, Tassou SA. A systematic review on the recent advances of the energy efficiency improvements in non-conventional food drying technologies. *Trends in Food Science & Technology* 2020;100:67 – 76. <http://www.sciencedirect.com/science/article/pii/S0924224419304558>.
- [3] Chasiotis VK, Tzempelikos DA, Filios AE, Moustris KP. Artificial neural network modelling of moisture content evolution for convective drying of cylindrical quince slices. *Computers and Electronics in Agriculture* 2020;172:105074. <http://www.sciencedirect.com/science/article/pii/S0168169919310713>.
- [4] Jomlapeletikul A, Wiset L, Duangkhamchan W, Poomsa-ad N. Model-based investigation of heat and mass transfer for selecting optimum intermediate moisture content in stepwise drying. *Applied Thermal Engineering* 2016;107:987 – 993. <http://www.sciencedirect.com/science/article/pii/S1359431116311954>.
- [5] Sritongtae B, Morgan MRA, Duangmal K. Drying kinetics, physico-chemical properties, antioxidant activity and phenolic composition of foam-mat dried germinated rice bean (*Vigna umbellata*) hydrolysate. *International Journal of Food Science & Technology* 2017;52(7):1710–1721. <https://ifst.onlinelibrary.wiley.com/doi/abs/10.1111/ijfs.13401>.
- [6] Kumari B, Tiwari BK, Hossain MB, Rai DK, Brunton NP. Ultrasound-assisted extraction of polyphenols from potato peels: profiling and kinetic modelling. *International Journal of Food Science & Technology* 2017;52(6):1432–1439. <https://ifst.onlinelibrary.wiley.com/doi/abs/10.1111/ijfs.13404>.
- [7] Shi L, Gu Y, Wu D, Wu X, Grierson D, Tu Y, et al. Hot air drying of tea flowers: effect of experimental temperatures on drying kinetics, bioactive compounds and quality attributes. *International Journal of Food Science & Technology* 2019;54(2):526–535. <https://ifst.onlinelibrary.wiley.com/doi/abs/10.1111/ijfs.13967>.
- [8] López-Ortiz A, Méndez-Lagunas LL, Delesma C, Longoria A, Escobar J, Muñoz J. Understanding the drying kinetics of phenolic compounds in strawberries: An experimental and density functional theory study. *Innovative Food Science & Emerging Technologies* 2020;60:102283. <http://www.sciencedirect.com/science/article/pii/S1466856419306964>.

- [9] Lusas EW, Rooney LW. *Snack Foods Processing*. CRC Press; 2001. [https://books.google.com.mx/books?id=W\\_5wlzckPkMC](https://books.google.com.mx/books?id=W_5wlzckPkMC).
- [10] Demarchi SM, Irigoyen RMT, Giner SA. Vacuum drying of rosehip leathers: Modelling of coupled moisture content and temperature curves as a function of time with simultaneous time-varying ascorbic acid retention. *Journal of Food Engineering* 2018;233:9 – 16. <http://www.sciencedirect.com/science/article/pii/S0260877418301389>.
- [11] Welsh ZG, Khan MIH, Karim MA. Multiscale modeling for food drying: A homogenized diffusion approach. *Journal of Food Engineering* 2021;292:110252. <http://www.sciencedirect.com/science/article/pii/S0260877420303435>.
- [12] Mujumdar AS. *Handbook of industrial drying*, fourth edition. CRC Press; 2014.
- [13] López-Ortiz A, Rodríguez-Ramírez J, Méndez-Lagunas LL, Martynenko A, Pilatowsky-Figueroa I. Non-isothermal drying of garlic slices (*Allium sativum*, L.): Wave period and initial temperature of the heating/cooling effect. *Food and Bioprocesses Processing* 2018;111:83 – 92. <http://www.sciencedirect.com/science/article/pii/S0960308518304073>.
- [14] Diamante LM, Munro PA. Mathematical modelling of the thin layer solar drying of sweet potato slices. *Solar Energy* 1993;51(4):271 – 276. <http://www.sciencedirect.com/science/article/pii/0038092X93901225>.
- [15] Gulcimen F, Karakaya H, Durmus A. Drying of sweet basil with solar air collectors. *Renewable Energy* 2016;93:77 – 86. <http://www.sciencedirect.com/science/article/pii/S0960148116301343>.
- [16] Azaizia Z, Kooli S, Elkhadraoui A, Hamdi I, Guizani A. Investigation of a new solar greenhouse drying system for peppers. *International Journal of Hydrogen Energy* 2017;42(13):8818–8826. <https://www.sciencedirect.com/science/article/pii/S0360319916316895>.
- [17] Sonmete MH, Mengeş HO, Ertekin C, Ozcan MM. Mathematical modeling of thin layer drying of carrot slices by forced convection. *Journal of Food Measurement and Characterization* 2017;.
- [18] Zhu A, Zhao J, Wu Y. Modeling and mass transfer performance of *Dioscorea alata* L. slices drying in convection air dryer. *Journal of Food Process Engineering* 2020;43(7):e13427. <https://onlinelibrary.wiley.com/doi/abs/10.1111/jfpe.13427>.
- [19] Mujumdar AS. *Fundamental principles of drying*; 2000.
- [20] Ertekin C, Firat MZ. A comprehensive review of thin-layer drying models used in agricultural products, *Critical Reviews in Food Science and Nutrition*. *Critical Reviews in Food Science and Nutrition* 2017;57:701–717. <https://www.tandfonline.com/doi/full/10.1080/10408398.2014.910493>.
- [21] Wang DC, Fon DS, Fang W, Sokhansanj S. Development of a Visual Method to Test the Range of Applicability of Thin Layer Drying Equations Using MATLAB Tools. *Drying Technology* 2004;22(8):1921–1948. <https://doi.org/10.1081/DRT-200032878>.
- [22] Erbay Z, Icier F. A Review of Thin Layer Drying of Foods: Theory, Modeling, and Experimental Results. *Critical reviews in food science and nutrition* 2010;50:441–64.
- [23] Thongcharoenpipat C, Yamsaengsung R. Improving the drying kinetics and microstructure of vacuum-fried ripened durian chips. *International Journal of Food Science & Technology* 2022;57(5):2862–2871. <https://ifst.onlinelibrary.wiley.com/doi/abs/10.1111/ijfs.15547>.
- [24] Yarahmadi N, Hojjatoleslamy M, Sedaghat Boroujeni L. Different drying methods of *Pistacia Atlantica* seeds: Impact on drying kinetics and selected quality properties. *Food Science & Nutrition* 2020;8(7):3225–3233. <https://onlinelibrary.wiley.com/doi/abs/10.1002/fsn3.1582>.
- [25] Wuytack L. Pade Approximation and its Applications. In: *Proceedings of a Conference held in Antwerp, Belgium*; 1979. p. 396.

- [26] Del Río JA, Zimmerman RW, Dawe RA. Formula for the conductivity of a two-component material based on the reciprocity theorem. *Solid State Communications* 1998;106:183–186. <https://www.sciencedirect.com/science/article/abs/pii/S0038109898000519>.
- [27] Kumar A, Saboo S, Shet S, Pilehavari A, Serth R. Correlation of rheometric data and hydraulic calculations using rational polynomials. *Chemical Engineering Communications* 2000;183:99–117. <https://www.tandfonline.com/doi/abs/10.1080/00986440008960504>.
- [28] Nunez-Santiago MC, Santoyo E, Bello-Perez LA, Santoyo-Gutierrez S. Rheological evaluation of non-Newtonian Mexican nixtamalised maize and dry processed masa flours J. *Journal of Food Engineering* 2003;60:55–66. <https://www.sciencedirect.com/science/article/abs/pii/S0260877403000189?via%3Dihub>.
- [29] Wong-Loya JA, Andaverde J, Santoyo E. A new practical method for the determination of static formation temperatures in geothermal and petroleum wells using a numerical method based on rational polynomial functions. *Journal of Geophysics and Engineering* 2012;9:711–728. <https://academic.oup.com/jge/article/9/6/711/5127427>.
- [30] Wong-Loya JA, Santoyo E, Andaverde JA, Quiroz-Ruiz A. RPM-WEBBSYS: A web-based computer system to apply the rational polynomial method for estimating static formation temperatures of petroleum and geothermal wells. *Computers and Geosciences* 2015;85:45–59. <https://www.sciencedirect.com/science/article/pii/S009830041530042X?via%3Dihub>.
- [31] Del Río-Portilla JA, Andaverde-Arredondo JA, Wong-Loya JA, Sistema y método de obtención de parámetros termodinámicos en situaciones transitorias que tienden a valores de saturación.; 2018.
- [32] Andaverde J, Wong-Loya JA, Vargas-Tabares Y, Robles-Perez M. A practical method for determining the rheology of drilling fluid. *Journal of Petroleum Science and Engineering* 2019;180:150–158. <https://www.sciencedirect.com/science/article/abs/pii/S0920410519304930>.
- [33] Owen TH, Orville CS. *Computational Methods in Chemical Engineering*, first edition. Englewood Cliffs; 1995.
- [34] Seyed-Hassan M, Alireza S, Mahmood Reza G. Analyzing drying characteristics and modeling of thin layers of peppermint leaves under hot-air and infrared treatments. *Information Processing in Agriculture* 2017;4(2):128–139. <https://www.sciencedirect.com/science/article/pii/S2214317317300100?via%3Dihub>.
- [35] López-Ortiz A, Rodríguez-Ramírez J, Méndez-Lagunas L. Effects of Drying Air Temperature on the Structural Properties of Garlic Evaluated During Drying. *International Journal of Food Properties* 2013;16(7):1516–1529. <https://doi.org/10.1080/10942912.2011.599090>.
- [36] Román-Roldán NI, López-Ortiz A, Ituna-Yudonago JF, García-Valladares O, Pilatowsky-Figueroa I. Computational fluid dynamics analysis of heat transfer in a greenhouse solar dryer “chapel-type” coupled to an air solar heating system. *Energy Science & Engineering* 2019;7(4):1123–1139. <https://onlinelibrary.wiley.com/doi/abs/10.1002/ese3.333>.
- [37] Castillo-Tellez M, Pilatowsky-Figueroa I, Castillo-Téllez B, López-Vidaña EC, López-Ortiz A. Solar drying of Stevia (*Rebaudiana Bertoni*) leaves using direct and indirect technologies. *Solar Energy* 2018;159:898 – 907. <http://www.sciencedirect.com/science/article/pii/S0038092X17310149>.
- [38] Nair PK, Espinosa-Santana AL, Guerrero-Martínez L, López-Ortiz A, Nair MTS. Prospects toward UV-blue filtered solar drying of agricultural farm produce using chemically deposited copper chalcogenide thin films on cellular polycarbonate. *Solar Energy* 2020;203:123 – 135. <http://www.sciencedirect.com/science/article/pii/S0038092X2030387X>.
- [39] Estrada-Wiese D, Del Río-Chanona EA, Del Río JA. Stochastic optimization of broadband reflecting photonic structures. *Sci. Rep.* 8.; 2010.
- [40] Estrada-Wiese D, Del Río-Chanona EA, Del Río JA. Stochastic optimization of broadband reflecting photonic structures. *Rev Mex Fisica* 2018;64:72–81.